Effect of van der Waals interaction on energetics and transport properties of a single anthracene molecule adsorbed or confined inside a carbon nanotube

L. Debbichi, Y. J. Dappe, and M. Alouani

Institut de Physique et Chimie des Matériaux de Strasbourg, UMR 7504, CNRS–Université de Strasbourg, F-67034 Strasbourg, France

(Received 6 October 2011; revised manuscript received 11 January 2012; published 23 January 2012)

The energetics and transport properties of a single aromatic molecule ($C_{14}H_{10}$) in interaction with a metallic single-walled carbon nanotube (SWCNT) have been studied using state-of-the-art density functional calculations. In both adsorption and encapsulation configurations, we show that the fundamental importance of the weak van der Waals (vdW) interactions is to stabilize the position of the molecule. These interactions have been treated through the *ab initio* linear combination of atomic orbitals (LCAO-S^2) method including the vdW weak interactions. Moreover, we show that the electric conductance of the SWCNT, calculated within a nonequilibrium Green's-function formalism, is very sensitive to the position of the molecule with respect to the nanotube. The change of the conductance is explained in terms of charge transfer strength between the nanotube and the molecule.

DOI: 10.1103/PhysRevB.85.045437 PACS number(s): 71.20.Tx, 73.22.−f

I. INTRODUCTION

The modifications of the intrinsic properties of single-walled carbon nanotubes (SWCNT) by defects, doping, or external perturbations are keys for engineering of new devices. In addition to the fundamental understanding of electronic and transport properties in the SWCNT, the tuning of their intrinsic electronic properties by chemical doping,[1,2] π stacking,[3,4] or functionalization[5] improves their potential for technological applications. SWCNTs are considered to be an extended π electron system and can combine with other π electron systems, such as aromatic molecules, via π stacking interaction.[6] Doping of SWCNTs with organic molecules has opened new routes for the fabrication of hybrid nanostructures.[7] In that manner SWCNTs can be filled with different compounds affecting their physical properties. It has been shown, for example, that encapsulated C_{60} molecules and metallofullerenes can modify the local electronic structure of nanotubes.[8,9] In this regard, SWCNTs can also be used for atoms or small molecules storage,[10] as has been proposed for hydrogen.

The stable and controlled encapsulation of organic molecules inside SWCNTs has been achieved experimentally, and it was found that the organic molecules predominantly occupy the inner space of the nanotube.[11] However, there are no *ab initio* calculations about the stabilization of organic molecules inside the SWCNTs where the weak van der Waals (vdW) interactions are considered. This is mainly due to the complexity of the van der Waals interaction, which is weak and long ranged compared to covalent bonding, which is strong and short ranged. It is therefore difficult to describe accurately both types of interactions within the same theoretical framework, and only recently are some approaches becoming available within density functional theory (DFT).[12–16] In this paper, we present results of encapsulation of an anthracene molecule on a SWCNT and the adsorption on its surface. The physics to convey is on the effect of the vdW interaction on the stabilization of the position of the anthracene molecule on a SWCNT as well as its effect on the electric conductance. We will show that without the vdW weak interaction the molecule is not adsorbed on a SWCNT and has no stable position inside the nanotube. Once the molecule is stabilized by the vdW weak interaction, we calculate the conductance of the SWCNT with or without the interaction with this molecule. We show, in particular, that the presence of the molecule leads to a reduction of the conductance.

II. COMPUTATIONAL DETAILS

Our standard DFT calculations of the structural and electronic properties, as well as of the electric conductance, have been performed using the *ab initio* SIESTA code[17] within the local-density approximation (LDA) as parametrized by Perdew and Zunger.[18] The core electrons were replaced by nonlocal norm-conserving pseudopotentials.[19] A double-zeta, single-polarization basis (DZP) set of localized atomic orbitals[20] has been used for the valence electrons. An energy cutoff of 300 Ry for the grid integration was utilized to represent the electron charge density. Our calculations were performed using a supercell technique. To avoid any interaction between the nanotubes of different unit cells, we increased the center-to-center distance between nearest nanotubes to 25 Å. For all the calculations we have used 8 unit cells of SWCNT (10,10) with a total length of 19.747 Å. We have found that at this length of supercell there is no direct interaction of the molecule with its supercell images. In all the electronic properties calculations, $1 \times 1 \times 32$ special k points[21] were used to sample the one-dimensional Brillouin zone. To make the **k**-point integration in the Brillouin zone we have used a Gaussian smearing of 0.1-eV width at half maximum. At the LDA level, the structure optimization, i.e., the atomic positions, and the lattice constants were relaxed following the Hellman-Feynman theorem, using a conjugate gradient method, until the average force exerted on an atom became less than 0.04 eV/Å. The transport properties of the carbon nanotube have been determined using the nonequilibrium Green's-function method (NEGF) as implemented in the SMEAGOL code.[22,23]

For the vdW and weak interaction between the molecule and the nanotube, we have used the FIREBALL code[24–26] with the implementation of the linear combination of atomic orbitals (LCAO-S^2) + vdW formalism.[13,14] The FIREBALL, like the

 ©2012 American Physical Society

SIESTA code, is an *ab initio* molecular dynamics tight-binding code that uses truncated numerical orbitals defined by a spatial cutoff radius. This method uses an LDA approach in the frame of the self-consistent Harris functional, and the core electrons were also replaced by nonlocal norm-conserving pseudopotentials.[19] Here we have used an optimized $2s2p$ orbital basis set for the carbon atoms and an optimized $1s$ orbital for hydrogen.[27] In the LCAO-S^2 + vdW approach, previously developed for noble gases[28] and applied to different SWCNT systems,[14,29,30] we have taken into account two contributions that aim to give the equilibrium of the weak interaction. First, we consider the weak chemical interaction, which is due to the small overlaps between the electronic densities. In fact, it can be seen as a "small" covalence, leading in the present case to a repulsive interaction. This interaction is treated in perturbation, using an expansion of the electronic wave functions with respect to the overlaps. This expansion is based on a development in S^2 (since in the weak interaction case the overlaps are really small) of the $S^{-1/2}$ term appearing in the Löwdin orthogonalization. This orthogonalization effect induces a shift of the occupied eigenenergies of each independent subsystem, leading to a repulsion energy between them. This shift is defined as

$$\delta^S \varepsilon_n = -\sum_m \frac{1}{2}[S_{nm}T_{mn}+T_{nm}S_{mn}]+\frac{1}{4}\sum_m |S_{nm}|^2(\varepsilon_n - e_m),$$
$$\delta^S e_m = -\sum_n \frac{1}{2}[S_{mn}T_{nm}+T_{mn}S_{nm}]+\frac{1}{4}\sum_n |S_{nm}|^2(e_m - \varepsilon_n), \quad (1)$$

where S_{nm} and T_{mn} are the overlap and hopping integrals, respectively, between eigenvectors e_m and ε_n in the two interacting subsystems, i.e., the molecule and the SWCNT, respectively. The effect of the hopping T_{mn} matrix elements can be calculated in a standard intermolecular second-order perturbation theory:

$$\delta^T \varepsilon_n = \sum_m \frac{|T_{mn}|^2}{\varepsilon_n - e_m}, \quad \delta^T e_m = \sum_n \frac{|T_{mn}|^2}{e_m - \varepsilon_n}. \quad (2)$$

Thus, we obtain the following weak chemical contribution to the interaction energy:

$$E_{\text{weak chemical}} = 2\sum_{n=\text{occ.}} (\delta^S \varepsilon_n + \delta^T \varepsilon_n) + 2\sum_{m=\text{occ.}} (\delta^S e_m + \delta^T e_m), \quad (3)$$

where a factor of 2 has been included to take into account the spin degeneracy and only filled states are considered.

The second contribution is the vdW interaction itself, arising from charge fluctuations in the interacting subsystems, fluctuations that lead to electronic dipoles. In the frame of the dipolar approximation, we consider the interaction between the dipoles from two atoms, one of each subsystem. This interaction is calculated for each pair of atoms between the interacting subsystems and added in perturbation. Practically, we first calculate every subsystem independently in standard DFT in order to get the initial molecular levels as well as the overlaps and hopping between the two subsystems. Then we evaluate the weak chemical and the vdW energy in perturbations.

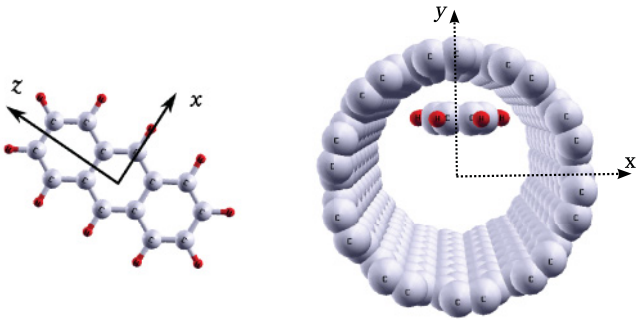

FIG. 1. (Color online) Structure of the isolated anthracene molecule and its encapsulation inside the (10,10) SWCNT.

Finally, the balance between these two contributions gives us the equilibrium position of the anthracene in the SWCNT as well as its binding energy. Notice that the weak interactions are not included in the potential, and therefore we do not have access to the corresponding forces. Consequently, for minimum-energy determination, we have to set up different geometrical configurations and calculate the corresponding total energies.

III. RESULTS

In this section we will discuss the results obtained for the equilibrium position of the anthracene molecule in interaction with a (10,10) SWCNT. We consider the configurations of both the adsorption and the encapsulation cases. Figure 1 presents the geometry of the encapsulation calculation.

We consider first the stability of the molecule adsorbed on the SWCNT. In this study, we have varied the molecule-nanotube distance and have calculated the binding energy E_b at each position, using either LDA or our LCAO-S^2 + vdW formalism. The results are presented in Fig. 2, where we show the evolution of the binding energy of the adsorbed anthracene molecule as a function of the molecule-nanotube distance. These results clearly indicate that no interaction is found within the LDA, whereas when the vdW interaction is considered, a clear minimum appears at 3 Å. Focusing on this minimum, we have determined the electronic density of states (DOS) of the system and compared it with the one of the pristine SWCNT.

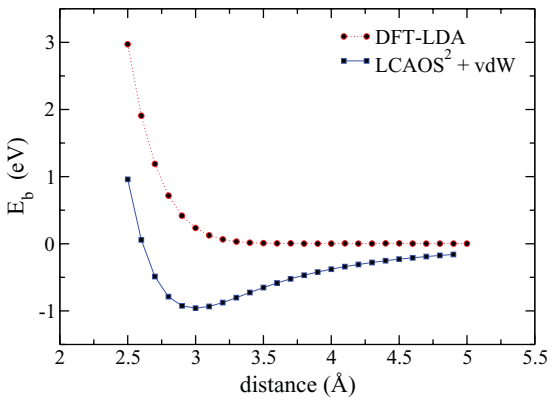

FIG. 2. (Color online) Binding energy (in eV) of the molecule adsorbed on the SWCNT (10,10) as a function of the distance. The red curve (light gray) represents the LDA result, while the blue curve (dark gray) represents the LCAO-S^2 + vdW energy.

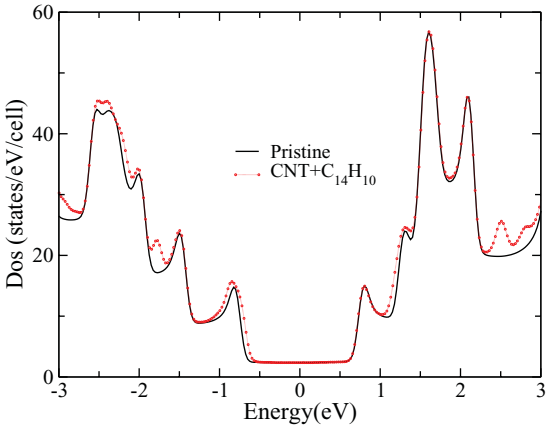

FIG. 3. (Color online) DOS comparison of the isolated (pristine) SWCNT (black curve) and the adsorbed molecule SWCNT [dashed red (gray) curve].

In the results presented in Fig. 3, it can be seen that there is practically no difference in DOS at the vicinity of the Fermi level, indicating that transport properties will not be affected by the adsorption of the anthracene molecule.

We now consider the case of the encapsulated molecule inside the SWCNT. The LDA full relaxation showed that the molecule remained parallel to the xz plane. Since our vdW method is based on total-energy minimization, we have constrained the molecule to be parallel to the xz plane. We first positioned the molecule along the tube axis and moved it along the x direction, and then for every x position we moved it along the y direction. Once we found that the molecule is stable at $x = 0$ and $y = 3.3$ Å (see Fig. 4), we rotated the molecule around the y axis to look for the most stable position.

In Fig. 4 we observe the energy variation of the anthracene molecule in the SWCNT (10,10) by moving it along the diameter (x axis). Along this path, the molecule presents two minima, which represent, in fact, a circular minimum inside the SWCNT. These minima arise from the balance between the attractive and the repulsive interactions of the SWCNT, in good agreement with a previous result on the peapod structure.[14] Of course these two minima would be converted into a unique one along the SWCNT axis if we were considering a smaller diameter for the tube. In the second part of Fig. 4, we represent the same energy variations by fixing several x positions and moving the molecule along the y coordinate. Here as well we can observe the appearance of such a circular minimum, except when considering the x coordinate over 1.1 Å, where there is practically no attraction. In that case, the anthracene is already too close to the nanotube wall, yielding an important repulsion that prohibits the apparition of a minimum.

Figure 5 represents the energy evolution of the molecule encapsulated inside the SWCNT under a rotation along the y axis, starting from a position along the SWCNT axis (0°) to a position orthogonal to that axis (90°). This evolution is important for transport purpose since the relative orientation of the molecule in the nanotube will affect significantly the conductance of the total system. In order to stress the influence of the vdW weak interactions on the behavior of the system, we have calculated the evolution of this binding energy in standard LDA as well as with the LCAO-S^2 + vdW method. The LDA result (red line with circles in Fig. 5) does not show any significant minimum. We can only observe a strong repulsion between 60° and 90°, i.e., repulsion that goes to zero around 40°, but with no clear minimum. Therefore, according to the LDA result, the anthracene molecule is not bonded to the nanotube, which lets us expect no significant interaction and, consequently, no influence on transport properties. On the contrary, from the blue curve with squares that includes the weak vdW interactions, we can roughly observe the same evolution, but with a clear minimum of ∼0.35 eV at about 40°. In fact, the direct comparison between the two curves reveals a well-known fact, which is the exponential decay of the DFT-LDA calculation with distance and the inability to describe properly the weak interactions like van der Waals. In the present case, the molecule goes farther from the SWCNT wall by rotating between 0° and 60°. At about 40°, the balance between attraction and repulsion in the LCAO-S^2 + vdW approach gives rise to an equilibrium position of the molecule.

Considering this behavior, we now present the results of electronic structure and conductance calculations at the equilibrium position and also in the case of a strong repulsive configuration, around 80°, in order to correlate the difference in the strengths of interaction with the calculated electric conductances.

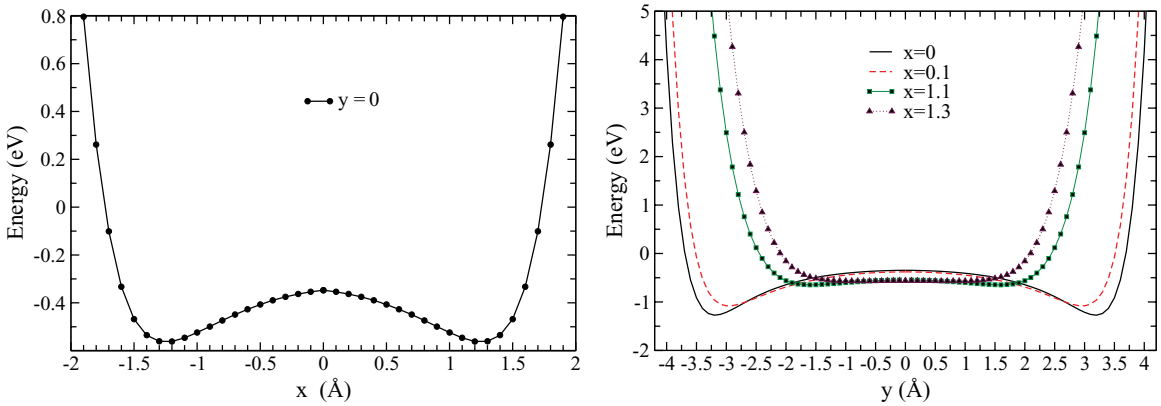

FIG. 4. (Color online) Total energy of the system of the system anthracene molecule encapsulated inside the SWCNT (10,10) (left) as a function of its position along the x direction, as shown in Fig. 1, and (right) as a function of the y direction for different positions along the x direction (from top to bottom $x = 0$, $x = 0.1$, $x = 1.1$ and $x = 1.3$ Å). The molecule shows a global minimum for x=0 and $y = 3.3$ Å.

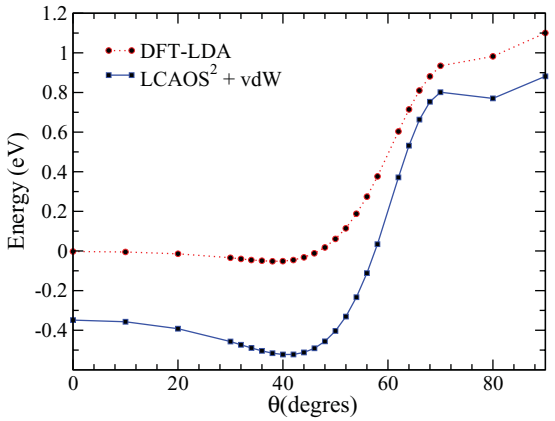

FIG. 5. (Color online) Binding energy (eV) of the anthracene molecule encapsulated inside the SWCNT as a function of the orientation angle in the (x, z) plane. The red curve with circles represents the LDA result, and the blue curve with squares represents that obtained by means of the LCAO-S^2 + vdW method.

The electronic band structure and the DOS near the Fermi level for these two configurations are represented in Figs. 6 and 7, respectively. we can observe a slight modification of the band structure in the fundamental configuration for either the valence or conduction band of the SWCNT. This is attributed to the degeneracy removal of the energy bands in the SWCNT with the molecule-tube interaction. On the other hand, at 80° the band splitting is more pronounced because the molecule interacts more with the SWCNT. There is even a small band gap due to Pauli repulsion of the two crossing bands of the same symmetry along the Γ-X direction. We notice also the presence of a flat band at about −0.4 eV below the Fermi level due mainly to the highest occupied molecular orbital (HOMO) of the anthracene molecule. This flat band is further pushed toward higher energies when the molecule is further rotated ($\theta = 80°$). This energy shift is due to the strong interaction with the nanotube and is clearly seen in the calculated conductance (see the calculated transmission). Notice that increasing the size of the supercell will not change

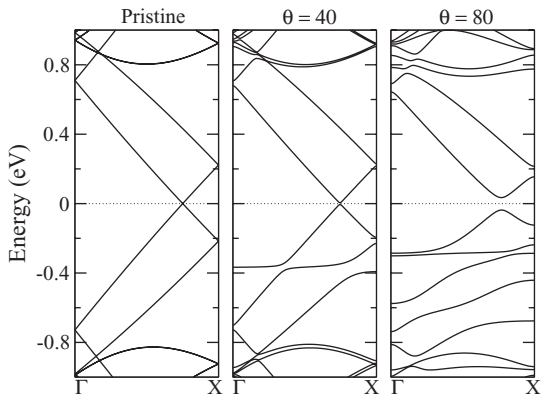

FIG. 6. Comparison of the band structures of (left) the isolated pristine SWCNT with those of the encapsulated molecule inside the SWCNT, where the molecule is rotated by (middle) 40° and (right) 80°, respectively. Notice the presence of the flat band near −0.4 eV due mainly to the presence of the HOMO of the anthracene molecule.

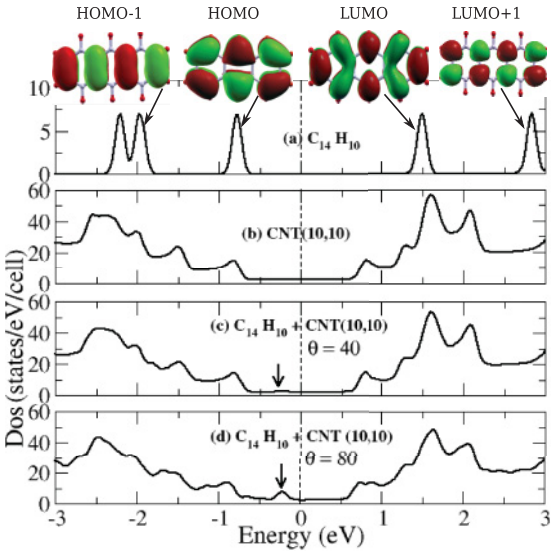

FIG. 7. (Color online) Comparison of the DOS of (a) the isolated anthracene molecule, (b) the isolated SWCNT, (c) the SWCNT + anthracene at 40°, and (d) at 80°. The character of the two highest occupied molecular orbitals (HOMO) and the two lowest unoccupied molecular orbitals (LUMO) are also shown

the position of flat bands since the interaction of the molecule with its supercell images is negligible for this size of the supercell. However, the increase of the supercell will add additional folding of the bands along the Γ-X direction due to the reduction of the size of the one-dimensional Brillouin zone. Mulliken population analysis shows, indeed, that there is a charge transfer from the nanotube to the molecule of 0.6 electron for $\theta = 40°$ and 1.05 electrons for $\theta = 80°$. The charge transfer is much larger for $\theta = 80°$ because the molecule is closer to the nanotube (the smallest distance between them is about 1.01 Å, via the hydrogen bond).

Figure 7 presents the DOS of the isolated SWCNT (10,10) and anthracene molecule and of the SWCNT encapsulating the molecule in the two configurations, i.e., at 40° and 80°. The charge distributions of the two highest valence states and the two lowest conduction states are also shown, and they show how the molecule will interact with the SWCNT. We find that the DOS of the combined system in both configurations differs from the simple superposition of its components, indicating some degree of interaction between the molecule and the nanotube. As expected from the band splitting observed in Fig. 6, the DOS of the molecule at 40° presents a new peak at ∼0.35 eV in the valence part. This is similar to what is observed in a boron-doped armchair carbon nanotube.[2] As will be seen later, this new peak changes the electric conductance of the nanotube. In the case of strong interaction (molecule at 80°) the electronic structure of the nanotube is strongly modified since it shows a stronger peak in the plateau (shown by an arrow) of the DOS above the maximum valence band. It is clear that the molecule SWCNT interaction increases the peak height. Indeed, for the broad peak appearing between −0.43 and −0.35 eV, its corresponding intensity is greater than the peak when the molecule is at 40° with respect to the SWCNT. Beyond this region the DOS is very similar to that of the isolated SWCNT. When the molecule is rotated by

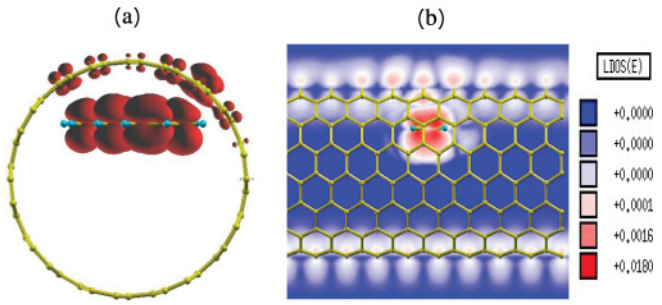

FIG. 8. (Color online) Local density of the molecule in the fundamental configuration (40°) in $E = E_F - 0.38$ eV: (a) isosurface at 2.10^{-4} electron/bohr^3 and (b) local-density profile in lateral view.

80°, the interaction between the molecule and the nanotube increases, and the shape of the DOS is greatly changed. As a consequence, two intense peaks in the plateau of the DOS appear. The increase of the peaks is due to the excess charge transfer of 1.05 electrons toward the molecule. However, even the first peak of the DOS of the anthracene molecule is outside the plateau of the DOS of the nanotube. Its interaction with the nanotube occurs at the vicinity of the Fermi level, contrary to what was observed with the adsorption of the molecule on the wall of the nanotube.

The coupling between a nanotube and aromatic molecule can be further investigated by local-density analysis around the observed new peaks in the plateau of the DOS. Figures 8 and 9 display the isovalue of local density in Figs. 8(a) and 9(a) and local density profile in the plane tangent to the tube wall in Figs. 8(b) and 9(b). The delocalization of π conduction electron over the molecule and some atoms in the nanotube is clearly shown in these two configurations, but it is more intense when the molecule is in the repulsive region. A similar effect is found for the noncovalent functionalization of a carbon nanotube with an aromatic molecule,[10] indicating that the hybridization of π electrons between nanotubes and molecules is the common feature of all aromatic molecules adsorbed or encapsulated on nanotubes.

We show in Fig. 10 a comparison of the transmission coefficients for the isolated pristine SWCNT and the combined SWCNT-molecule system at 40° and 80°. As is well known, the isolated pristine SWCNT presents a transmission of $2G_0$, with $G_0 = 2e^2/h$ being the quantum of conductance. In Fig. 10, we can observe the reduction of conductance from $2G_0$ to $1G_0$ at the new energy levels induced by the coupling between the molecule and nanotube. These localized states seen in the

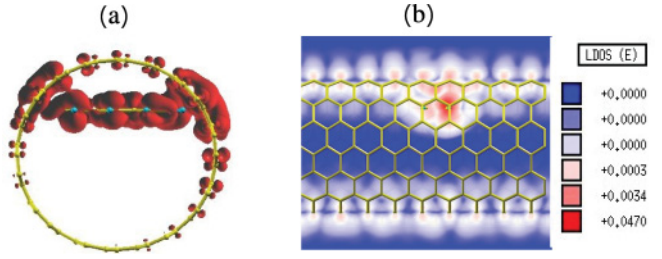

FIG. 9. (Color online) Local density of the molecule in the repulsive configuration (80°) at $E = E_F - 0.35$ eV: (a) isosurface at 2.10^{-4} electron/bohr^3 and (b) local-density profile in lateral view.

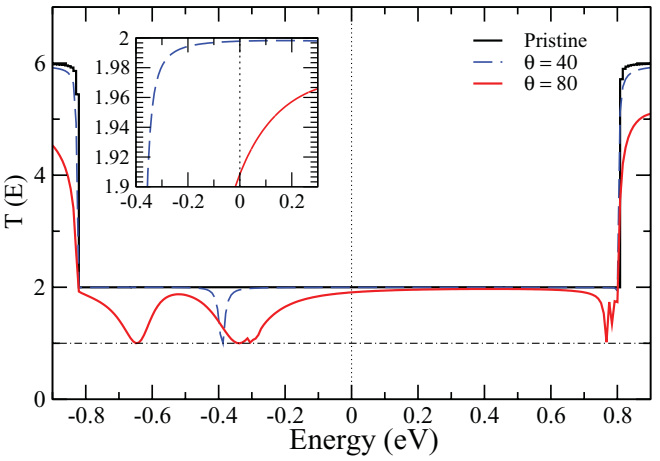

FIG. 10. (Color online) Comparison of transmission coefficients for the isolated SWCNT and for the combined system SWCNT + anthracene in the the two different configurations ($\theta = 40^\circ$ and 80°).

DOS profile can scatter an incoming conduction electron and thus reduce the conductance by one quantum conductance. This effect becomes greater when the molecule approaches the nanotube wall. In particular it clearly appears in Fig. 10 when the molecule varies from 40° to 80°. This reduction in the transmission is pushed toward higher energies for $\theta = 80°$ due to the strong interaction of the molecule with the nanotube. Notice that the small band gap in the band structure for $\theta = 80°$ has very little impact on the transmission (it is only slightly reduced compared to that for $\theta = 40°$). This is because the broadening of the density of states and the Green's function due to the 0.1-eV Gaussian width at half maximum smeared the band gap out completely (see Fig. 7).

IV. CONCLUSION

We have studied the interaction of the anthracene/metallic (10,10) SWCNT, when the molecule is adsorbed on or confined inside the nanotube. We have used different approaches in order to find the correct positions of the molecule in the nanotube. The LDA shows an energy curve that is totally flat, which means that the molecule does not interact with the nanotube. On the other hand, when the van der Waals interactions are included in the total-energy calculation, a clear minimum is obtained. The electronic structure calculations show the presence of new peaks in the plateau of the DOS caused by the interaction between the molecule and the nanotube when the molecule is confined inside the nanotube. These peaks are due to the interaction of the HOMO of the molecule with the electronic structure of the nanotube and to the resulting charge transfer from the nanotube to the anthracene molecule. These peaks cause the reduction of the conductance by one quantum conductance.

ACKNOWLEDGMENTS

M.A. and L.D. acknowledge partial support from an ANR pnano Grant No. ANR-06-NANO-053-01. This work was performed using HPC resources from GENCI-CINES Grant No. gem1100.

[1] A. H. Nevidomskyy, G. Csanyi, and M. C. Payne, Phys. Rev. Lett. **91**, 105502 (2003).
[2] H. J. Choi, J. Ihm, S. G. Louie, and M. L. Cohen, Phys. Rev. Lett. **84**, 2917 (2000).
[3] F. Tournus, S. Latil, M. I. Heggie, and J.-C. Charlier, Phys. Rev. B **72**, 075431 (2005).
[4] S. Latil, S. Roche, and J. C. Charlier, Nano Lett. **5**, 2216 (2005).
[5] A. Loópez-Bezanilla, F. Triozon, S. Latil, X. Blase, and S. Roche, Nano Lett. **9**, 940 (2009).
[6] J. Lu, S. Nagase, X. Zhang, D. Wang, M. Ni, Y. Maeda, T. Wakakara, T. Nakahodo, T. Tsuchiya, T. Akasaka, Z. Gao, D. Yu, H. Ye, W. N. Mei, and Y. Zhou, J. Am. Chem. Soc. **128**, 5114 (2006).
[7] L. LI, A. N. Khlobystov, J. G. Wltshire, G. A. D. Briggs, and R. J. Nicholas, Nat. Mater. **4**, 481 (2005).
[8] J. Lee *et al.*, Nature (London) **415**, 1005 (2002).
[9] D. J. Hornbaker, S. J. Kahng, S. Misra, B. W. Smith, A. T. Johnson, E. J. Mele, D. E. Luzzi, and A. Yazdani, Science **295**, 828 (2002).
[10] J. Zhao, A. Buldum, J. Han, and J. P. Lu, Nanotechnology **13**, 195 (2002).
[11] T. Takenobu, T. Takano, M. Shiraishi, Y. Murakami, M. Ata, H. Kataura, Y. Achiba, and Y. Iwasa, Nat. Mater. **2**, 683 (2003).
[12] D. C. Langreth, M. Dion, H. Rydberg, E. Schröder, P. Hyldgaard, and B. I. Lundqvist, Int. J. Quantum Chem. **101**, 599 (2005).
[13] Y. J. Dappe, M. A. Basanta, F. Flores, and J. Ortega, Phys. Rev. B **74**, 205434 (2006).
[14] Y. J. Dappe, J. Ortega, and F. Flores, Phys. Rev. B **79**, 165409 (2009).
[15] G. Savini, Y. J. Dappe, S. Öberg, J. C. Charlier, M. I. Katsnelson, and A. Fasolino, Carbon **49**, 62 (2011).
[16] S. Lebègue, J. Harl, T. Gould, J. G. Ángyán, G. Kresse, and J. F. Dobson, Phys. Rev. Lett. **105**, 196401 (2010).
[17] J. M. Soler, E. Artacho, J. D. Gale, A. GarcÃ-a, J. Junquera, P. Ordejón, and D. Sánchez-Portal, J. Phys. Condens. Matter **14**, 2745 (2002).
[18] J. P. Perdew and A. Zunger, Phys. Rev. B **23**, 5048 (1981).
[19] N. Troullier and J. L. Martins, Phys. Rev. B **43**, 1993 (1991).
[20] E. Artacho, D. Sánchez-Portal, P. Ordejón, A. García, and J. M. Soler, Phys. Status Solidi B **215**, 809 (1999).
[21] H. J. Monkhorst and J. D. Pack, Phys. Rev. B **13**, 5188 (1976).
[22] I. Rungger and S. Sanvito, Phys. Rev. B **78**, 035407 (2008).
[23] A. R. Rocha, V. M. García-Suárez, S. Bailey, C. Lambert, J. Ferrer, and S. Sanvito, Phys. Rev. B **73**, 085414 (2006).
[24] J. P. Lewis, K. R. Glaesemann, G. A. Voth, J. Fritsch, A. A. Demkov, J. Ortega, and O. F. Sankey, Phys. Rev. B **64**, 195103 (2001).
[25] P. Jelinek, H. Wang, J. P. Lewis, O. F. Sankey, and J. Ortega, Phys. Rev. B **71**, 235101 (2005); O. F. Sankey and D. J. Niklewski, *ibid.* **40**, 3979 (1989).
[26] J. P. Lewis, P. Jelinek, J. Ortega, A. A. Demkov, D. G. Trabada, B. Haycock, H. Wang, G. Adams, J. K. Tomfohr, E. Abad, H. Wang, and D. A. Drabold, Phys. Status Solidi B **248**, 1989 (2011).
[27] M. A. Basanta, Y. J. Dappe, P. Jelinek, and J. Ortega, Comput. Mater. Sci. **39**, 759 (2007).
[28] M. A. Basanta, Y. J. Dappe, J. Ortega, and F. Flores, Europhys. Lett. **70**, 355 (2005).
[29] M. Seydou, Y. J. Dappe, S. Marsaudon, J.-P. Aimé, X. Bouju, and A.-M. Bonnot, Phys. Rev. B **83**, 045410 (2011).
[30] M. Gicquel-Guézo, Y. J. Dappe, P. Turban, A. Moréac, H. Nong, S. Loualiche, Carbon **49**, 2971 (2011).